Modelling tyres wear: Local approach

Benoit Delattre, Rachel-Marie Pradeilles Duval, Claude Stolz

Modelling tyres wear: Local approach

B. Delattre[a,b], R.M. Pradeilles Duval[b] & C. Stolz[b]
[a]*LMS, Ecole Polytechnique, Palaiseau, France*
[b]*Manufacture des pneumatiques Michelin (MFPM), Clermont-Ferrand, France*

ABSTRACT: Mild wear of rubber-like materials in frictional contact is considered through particular abrasion patterns' study. A local constitutive law is introduced within geometrical and energetic considerations. Mesoscopic easily accessible experimental data are used to identify the material parameters. A local wear criterion is presented and two examples of wear parameters determination are presented, considering a classical phenomenological global wear model, Thomas' one. The purpose of this model is to be further implemented into finite element programs.

1 INTRODUCTION

A tyre surface is a rubber-like vulcanized filled system, which assures the junction between road and vehicle. Due to contact and tangential forces, wear can occur. Usual solicitations induce a slow tyre-scale homogeneous loss of material, called mild wear.

Mild wear of rubber-like materials is a microscopic and slow phenomenon regarding to the tyre size and dynamics. An accurate description of wear mechanisms (Archard 1957) has to be settled at appropriate scales, which are much smaller than the scale of a whole tyre. A phenomenological law for the rate of material loss (Schallamach 1954) at tyre scale leads to service life predictions but cannot describe the initiation and the evolution of wear in such a local scale. It is not appropriate to model abrasion patterns.

Wear phenomena are essentially characterized by a loss of materials; particles are taken off a sound solid. Unlike classical material, when submitted to repeated friction with hard antagonist, the surface of rubber-like materials roughens.

For different contact parameters (antagonist, pressure, sliding velocity, environment), rubber abrasion runs specific surface patterns (called abrasion patterns). In our case, we consider the patterns defined by periodic parallel ridges perpendicular to the sliding direction (Fig.1, (Petitet 2003)). This pattern is regarded as a signature of the wear phenomenon, depending on material and road properties.

We need to develop an intermediate model taking account of local wear patterns and structure-scale computation's requirements. This paper proposes a mesoscopic and homogenized model of wear and friction phenomena based on geometrical observations of abrasion patterns. This model will further be implemented in a numerical framework of local and continuous wear, not presented here.

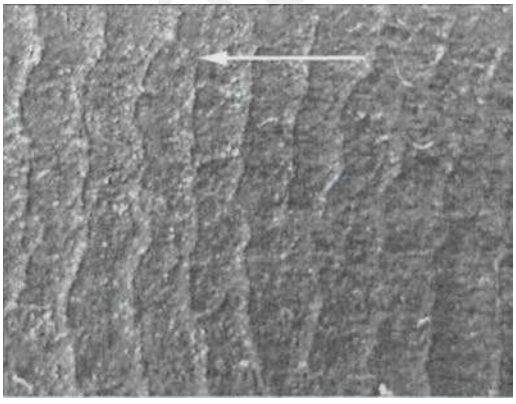

Figure 1. Example of a wrinkle type abrasion patterns, observed on tyre, sliding direction quoted by an arrow.

2 ON PATTERNS

The periodic parallel ridged pattern we consider is striking, at least for two reasons: it is inherent to mild wear of rubber-like materials (tyres, shoes, etc) and its geometric shape is conserved during cycling loading. For a sliding sphere (Petitet 2003) or a razor blade (Fukahori and Yamazaki 1994) on a rubber block, a rippled marked pattern is observed on the contact area, as early as the very first loading cycles.

The geometric features of these wrinkles, perpendicular to the sliding direction, are defined by their

width (l), their inter-ridge distance (d), their so-called wavelength ($\mathcal{L} = l + d$) and their height (h), which are constant in appearance on the surface (Fig.2(b)). Repeated sliding passes increase these features till they reach a critical size as shown in (Fukahori and Yamazaki 1994). In that case, two competing phenomena are observed: stick-slip oscillations and microvibrations during the frictional sliding phase. The wavelength of the initial wrinkles matches a natural period of the rubber according to the mean sliding velocity of the antagonist. The wavelength of the critical wrinkles matches the period of the stick-slip oscillations according to the mean sliding velocity.

The initial wrinkles, further called microridges according to their average wavelength ($\approx$10–100 μm), the critical wrinkles, further called ridges (mesoscopic-millimetric), the slider (from milli- to centimetric) and the slided length (decimetric) settle the length scales of the wear contact problem. We propose a mesoscopic scale model of a sliding hard indent on a block of rubber.

Petitet (Petitet 2003) does show it is possible to generate a microridged pattern with a spherical slider under peculiar experimental conditions with no stick-slip oscillations. In his experiments, the microridges do not develop towards ridges: the wrinkle geometrical features

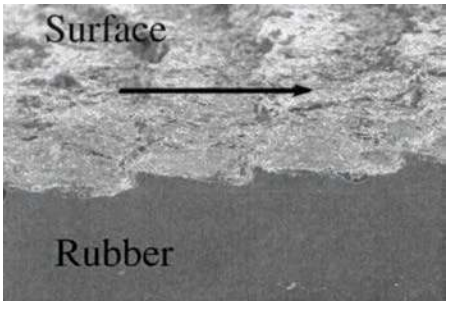

(a) Experimental example of a wrinkle

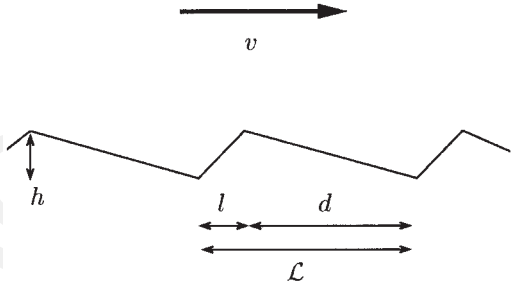

(b) Admissible model of a wrinkle

Figure 2. Wrinkles, pertinent features and representation, sliding direction quoted by an arrow.

(l_μ, d_μ, h_μ) remain steady. We note (l_ρ, d_ρ, h_ρ) the critical features observed in (Fukahori and Yamazaki 1994). Following Petitet's results, we describe microridged and ridged patterns separately even if they are related.

3 LOCAL BEHAVIOR

In accordance with Fig.3, the following settings are obtained. The loading and the block are symmetric with respect to (0_y) direction. Moreover, ridges and microridges are assumed to be spacially (0_y) invariant. Thus, we restrain to a 2D model in the plane (0, x, z), where ($0x$) is the sliding direction. The average height (in the direction $0z$) of the block at instant t is $q_m(t)$. The local difference of height to q_m(t) is $q(x,t)$, x is the eulerian abscissa. Let L denote the block's length, l_c the contact's length, υ the sliding velocity, λ the macroscopic loading parameters.

$q_m(t)$ is given by the global constitutive law of the material and we approximate the local motion by:

$$m\,\ddot{q}(x,t) + \eta\,\dot{q}(x,t) + k\,q(x,t) = f_\lambda(x,t,\lambda) \qquad (1)$$

where dotted letters ($\dot{q}$) represent time derivation, apostrophized letters (q') spacial derivation versus x, f_λ the loading function, which is unknown at this point just like the parameters η (which plays the role of viscosity), k (a local rigidity type quantity) and m. We only know that the solution of this equation is a wrinkle shape profile for $q(x,t)$.

In order to represent the relevant ridged patterns (Fig.2(a)) with $q_0(x,t)$, we have to solve an inverse problem consisting in: "Find (m, η, λ, f_λ) so that $q_0(x, t)$ is a solution of (Eq.1)?" The surface profile $q_0(x, t)$ is defined by its width l, its inter-ridge distance d and its height h, observed after an experiment defined by a given rubber-like block, a sliding velocity υ, a specific indentor and a prescribed pressure. For example, the profile (Fig.2(b)) is admissible to represent the pattern (Fig.2(a)).

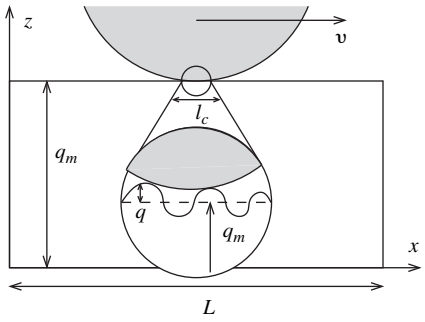

Figure 3. Sliding test and abrasion patterns' scale.

4 LOCAL CONTACT CONDITIONS

For general motion, we assume the following form f^{ρ}_{λ} for the loading f_{λ}:

$$f^{\rho}_{\lambda} = f^{\mu}_{\lambda} + f^{\sigma}_{\lambda} \tag{2}$$

$$f^{\mu}_{\lambda} = (\tau q' - \epsilon k q)\,\mathbb{H}(q') \tag{3}$$

$$f^{\sigma}_{\lambda} = A(\cos\frac{w_1\,x}{v} + \left(\cos\frac{w_2\,x}{v} - \cos\frac{w_1\,x}{v}\right)\mathbb{H}(q')) \tag{4}$$

where f^{μ}_{λ} represents the microvibrational part and f^{σ}_{λ} the stick-slip part ($\mathbb{H}$ is the Heaviside function, $\mathbb{H} = 0$ on $\mathbb{R}^*$, $\mathbb{H} = 1$ on $\mathbb{R}_+$). Further, the exposants μ, σ, ρ correspond respectively to the solutions of (Eq.1) where the loading f_{λ} is f^{μ}_{λ},f^{σ}_{λ},f^{ρ}_{λ}, the features without exposant are to be understood as general solution with any loading f_{λ} Considering the specific undeformed (Fig.4(a)) and deformed (Fig.4(b)) shape of a wrinkle, some authors explain implied wear mechanism is governed by shear loading specifically seen on the "tongue" of the ridge, the ridged excrescent part.

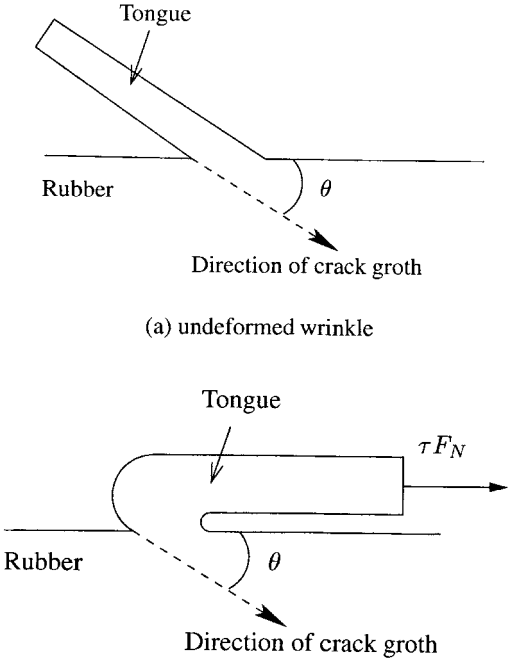

Figure 4. Local perturbation of contact condition on the wrinkles, F_N the normal contact effort.

The ridges are so deformed under the contact that they bend down, changing the local stiffness of the material. We do not comment now the different phenomenological mechanisms proposed, like abrasion of the tongues induced by fracture (Reznikovskii and Brodskii 1967) or fatigue cracks growth in tongue roots (Thomas 1975), we note simply the importance of the effective loading seen by the tongues. Then, we model this local variation of contact conditions by a small perturbation in elastic (ϵ) and shear (τ) modula on the tongue upper part (Fig.4(b)). Following (Xia 2003), we take account of a stick-slip motion with different stick (w_1) and slip (w_2) frequencies imposed directly into the loading.

The general solution of (Eq. 1) is

$$q(x,t) = \Lambda_s\, q_s(x) + \Lambda_\alpha\, q_\alpha(x,t) \tag{5}$$

where q_s is the steady solution per length unit and q_α a dumped solution per length unit, calculated by recurrence. The function q_s is spacially $\mathcal{L}$-periodic and q_α is spacially $\mathcal{L}$-pseudo-periodic; it has an increasing exponential part versus x and a decreasing one with respect to the time t.

5 ENERGY DISSIPATION

The energy release rate (or local dissipation) of the system (Stolz 2003), calculated on a period $\mathcal{L}$ can be written:

$$\mathcal{D}_{\mathcal{L}} = \left\langle \eta\dot{q}^2 - \tau q'\dot{q}\mathbb{H}(q') \right\rangle_{\mathcal{L}} \tag{6}$$

This quantity, integrated on the whole contact surface, gives the energy dissipation of the system at any moment. Three phenomena tend to make the system dissipate energy: friction, viscosity and wear. Experimentally, the mechanisms interact one to another and each effect can not be differentiated from the others. Besides, we assume that every part of $\mathcal{D}_{\mathcal{L}}$ can be identify mostly to a single phenomenon. The second part of the local dissipation $\mathcal{D}_{\mathcal{L}}$, noted $\mathcal{D}_{\{}$, linear to the shear modulus τ, takes into account the whole frictional dissipation of the system and some viscous effects. We do not tempt to fix the inter-dependency of both phenomena since we are preoccupied here with wear. Consequently, the first term in $\mathcal{D}_{\mathcal{L}}$ takes account of the whole wear dissipation.

To isolate the wear dissipation from dissipation induced by viscosity, we use the property that viscous effects tend to vanish at infinite time but material removal dissipates instantly. The q solution (Eq. 5) found in (Eq.6) has two contributions q_s and q_α. We have $\dot{q}_\alpha$ that tends to vanish with an infinite time like q_α. Then, we define the part of the dissipation exclusively due to wear as:

$$\mathcal{D}_w = \left\langle \eta(\Lambda_s\dot{q}_s)^2 \right\rangle_{\mathcal{L}} = \lim_{t\to\infty} \left\langle \eta\dot{q}^2 \right\rangle_{\mathcal{L}} \tag{7}$$

This term under-estimate the wear dissipation, because of the dependence between viscosity and wear dissipations. At this point, we have no reason to consider that the term $\mathcal{D}_\mathcal{L} - \mathcal{D}_w - \mathcal{D}_f$ is totally due to viscosity. We assume that the contribution of wear mechanisms in this dissipation is negligeable and that $\mathcal{D}_w$ is the whole wear energy release rate. The discussion upon the pertinency of this assumption follows in section 8.

6 WEAR CRITERION

Wear is a continuous loss of material. Experimentally, at any time, the same abrasion pattern is observed. Some regular wrinkles appear at the surface and grow till they reach a critical size. Then, their features remain steady even if the surface loses some material.

This mechanism is not an explanation but a signature of wear. We base a wear criterion on these experimental observations. In our model, the steady solution is given by $\Lambda_s q_s$. The increasing part of the facies is $\Lambda_\alpha q_\alpha$. To fit the observation, when the parameter Λ_s reaches the critical size h, the profile q remains at this mean level: the wrinkles cease to increase. On a period $\mathcal{L}$, the profile is meant to increase by the value Λ_α.

In our model, it means that for a sliding length of $\mathcal{L}$, when $\Lambda_s = h$, Λ_α represents the height of lost material. During that period, the wear dissipation is exactly:

$$\mathcal{D}_W = \eta h^2 \left\langle \dot{q_s}^2 \right\rangle_\mathcal{L} \tag{8}$$

For every $\mathcal{L}$ slide length, $\mathcal{D}_W$ is the energy release rate needed to lose some material, neglecting the initiation period of the wear phenomena (which appears in $\mathcal{D}_w$). Then the material loss rate is Λ_α. This criterion is local because it depends on the slide length seen at any point of the contact surface. To determine the global material loss on the surface, we have to integrate this criterion in time and in space, considering the local contact conditions. This criterion is a discretization of a continuous wear, compatible with a FEM computation. If a small elementary surface, S its area, slides on a length L, then the lost material volume is equal to $S\Lambda_\alpha L/\mathcal{L}$, when the energy release rate reaches the value $\mathcal{D}_W L/\mathcal{L}$.

7 PARAMETERS IDENTIFICATION

At mesoscopic scale, we have very few experimental data that can be both precise and accurate for macroscopic numerical simulations. However, the presented model seems to need a lot of parameters. In fact, to fit the experimental observations, the steady solution $\Lambda_s q_s$ of this model has to represent an admissible wrinkle (Fig.2) for a ridged abrasion pattern. Therefore, to identify the model's parameters, we use the geometrical features of abrasion patterns, seen as a signature of wear phenomena.

The identification process is divided in three steps. First, following Fukahori & Yamazaki (Fukahori and Yamazaki 1994) and Petitet (Petitet 2003) results, a microridge wear pattern is an experimental solution of wear mechanism, if there is no stick-slip solicitation. In our model, it means that when $f_\lambda = f^\mu_\lambda$, a microridge admissible profile (Fig.2), characterized by (l_μ, d_μ, h_μ), has to be a steady solution $\Lambda^\mu_s q^\mu_s$ to the model. We use the inherent relations to identify some material parameters.

Then, in the general case, the solution pattern is ridged, characterized by (l_ρ, d_ρ, h_ρ). Some stick-slip oscillations are observed, information we translate in $f_\lambda = f^\rho_\lambda$, because experimentally (Fukahori and Yamazaki 1994) the ridge pattern is a development of a microridge pattern. The steady solution $\Lambda^\rho_s q^\rho_s$ of this loading has to be a ridge admissible profile (Fig.2). The last material parameters are determined by these relations. Finally, we identify the wear criterion parameters by identification with a classical global wear criterion.

To summerize, the model counts 8 material and loading parameters (m, η, k, ϵ, τ, A, w_1, w_2) and 6 wear parameters (Λ^μ_s, Λ^μ_α, $\mathcal{D}^\mu_W$, Λ^ρ_s, Λ^ρ_α, $\mathcal{D}^\rho_W$). We assume that the data given by experience are (v, l_μ, d_μ, h_μ, l_ρ, d_ρ, h_ρ). The first data is the test's sliding velocity and the last 6 are given by a rugosimetric analysis of the contact surface.

7.1 *Microridge model*

The introduced microridge model presents a steady solution $\Lambda^\mu_s q^\mu_s$ if and only if the parameter ϵ follows the relation (Eq.9), that indicates the non explicit depends of q^μ_s in the parameter t. Now, if we assume the existence of that steady solution, it has to be pseudo-periodic like the microridge patterns it modelizes. Then, the parameter τ is fixed by the relation (Eq. 10) that comes from the equation $q^\mu_s(x) = q^\mu_s(x + \mathcal{L}^\mu)$. To represent an exact microridge model, the steady solution $\Lambda^\mu_s q^\mu_s$ has to match the observed quasi-steady microridge patterns, characterized experimentally by (l_μ, d_μ, h_μ). The two semi-periods are settled by (Eqs. 11–12), that impose the parameters k and η. There is an other relation upon the period $\mathcal{L}^\mu$ of the microridge pattern, but it did not give any information, in fact $\mathcal{L}^\mu = d_\mu + l_\mu$, which is a combination of (Eqs. 11–12).

To be accurate and experimentally pertinent, the microridge model has to respect the relations (Eq. 9–12). In these conditions, the theoretical pattern $\Lambda^\mu_s q^\mu_s$ (Fig.5), given by the model, fit the experimental microridge pattern, characterized by (l_μ, d_μ, h_μ).

$$\epsilon = \left(\frac{d_\mu}{l_\mu}\right)^2 - 1 \tag{9}$$

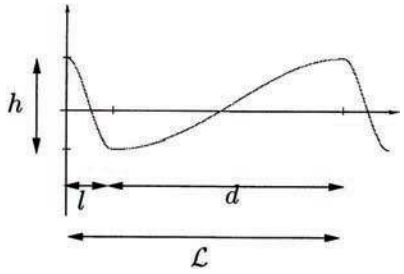

Figure 5. Solution profile of the model

$$\frac{\tau}{\eta\, v} = 1 + \frac{d_\mu}{l_\mu} \tag{10}$$

$$4k - \frac{(\eta v)^2}{mv^2} = m(\frac{2\pi v}{d_\mu})^2 \tag{11}$$

$$4k(1+\epsilon) - \frac{(\eta v - \tau)^2}{mv^2} = m(\frac{2\pi v}{l_\mu})^2 \tag{12}$$

7.2 *Complete model*

The steady solution $\Lambda_s^\rho q_s^\rho$ of the whole model has to match the observed quasi-steady critical ridge patterns. Given a pattern $\Lambda_s^\rho q_s^\rho$ (Fig.5), characterized experimentally by (l_ρ, d_ρ, h_ρ), we determine three independent relations between the parameters:

$$d_\rho = \frac{2\pi v}{w_1} \tag{13}$$

$$l_\rho = \frac{2\pi v}{w_2} \tag{14}$$

$$h_\rho = A \tag{15}$$

Once more, we have the relation on the period $\mathcal{L}^\rho = d_\rho + l_\rho$, linear combination of the first two equations that give the two semi-periods. As a matter of material and loading parameters, the model has exactly one degree of freedom, set as m.

7.3 *Wear parameters*

In fact, because the introduced model of wear is discrete, the two wear criteria, given by (Λ_s^μ, Λ_α^μ, $\mathcal{D}_W^\mu$) and (Λ_s^ρ, Λ_α^ρ, $\mathcal{D}_W^\rho$), have to be coherent to each other to represent an actual continuous mechanism. The difference between these two criteria is the period where they are calculated, $\mathcal{L}^\mu$ and $\mathcal{L}^\rho$. Then, we have the relation:

$$\mathcal{L}^\mu \mathcal{D}_W^\rho = \mathcal{L}^\rho \mathcal{D}_W^\mu \tag{16}$$

By definition, Λ_s^μ and Λ_s^ρ give the critical size of the wrinkle pattern for the microridge and ridge models respectively. So, we have:

$$\Lambda_s^\mu = h_\mu \tag{17}$$

$$\Lambda_s^\rho = h_\rho \tag{18}$$

It remains three wear parameters to identify: $\mathcal{D}_W^\rho$, Λ_α^μ and Λ_α^ρ. Experimentally, there is no proof that wear rates of a microridge and a ridge pattern are different. There is no proof of the opposite neither. We do not answer this question here, so, for now, we consider the way to identify Λ_α^μ is the same as to identify Λ_α^ρ, if they are different.

One interest of this model is to be computed in a finite element algorithm. The mechanism of wear is local and material loss rates can fluctuate on the whole contact surface. On the other hand, the measured material loss rates are macroscopic. It means that the experimental data used to fit our model are the material loss given here, integrated on space and time.

The only way to identify the wear parameters is to integrate our model on the contact surface for some fixed test conditions and to identify the whole lost material volume given by our model to experimental data or a classical phenomelogical wear criterion. For complex solicitations, FEM implementation is needed but we present here an simple example of analytical identification of our wear parameters to the Thomas model (Thomas 1975). This model considers a crack growing on a single ridge's basis, on the contrary to our continuous model of wear. The Thomas energy release rate, G, is given by the relation:

$$G = \frac{F_t}{L}(1+\cos\theta)^2 \tag{19}$$

and the abraded volume:

$$V = \beta L \sin\theta \left(\frac{F_t}{L}(1+\cos\theta)^\alpha\right) \tag{20}$$

with F_t the shear efforts, L the slide length, α and β some material coefficients, θ the angle of a surface crack.

We consider a single sliding spherical indentor, following the notations of (Fig.3), on a rubber block, which has been characterized for the Thomas model. The surface contact is S. The simplest integration of our model is when we assume an homogeneous material loss[1]. In these conditions, our model give the equations:

$$G = \frac{LS}{\mathcal{L}^\rho}\mathcal{D}_W^\rho \tag{21}$$

[1] This assumption is the worst we can make, because we lose the best contribution of our model, the localisation of wear.

$$V = \frac{SL\Lambda_\alpha^\rho}{\mathcal{L}^\rho} \tag{22}$$

The parameters of our local model are then identified to the global Thomas model, in the simplest homogeneous way. Now, considering that the wear in the center of the contact surface is more severe than in the edge (Petitet 2003) we precise our parameters.

For example, we can assume a simple Hertz distribution of the tangential shear, given by a Hertz law on the parameter m. The surface S is given by the contact radius a, $S = \pi a^2$. Then, the equations become:

$$G = \frac{L}{\mathcal{L}^\rho} \int_0^a \mathcal{D}_W^\rho r \, dr \tag{23}$$

$$V = \frac{a^2 L \pi \Lambda_\alpha^\rho}{4\mathcal{L}^\rho} \tag{24}$$

We emphasize that the parameter $\mathcal{D}_W^\rho$, given by (Eq. 8), is a complicated function of all the other parameters. In detail, $\mathcal{D}_W^\rho$ depends on the shear parameter τ and is increasing with the ridges' pseudo-period $\mathcal{L}^\rho$. Moreover, the link between Λ_α^ρ and $\mathcal{L}^\rho$ is not fixed by the present model and is the object of ongoing experimental research.

8 DISCUSSION

These examples of wear parameters identification are given here to understand the general method. The model will be accurate with a whole finite element model, which represents ongoing research. The point is that any phenomenological wear model can be identified with our model, the Thomas model being one of them. The present model do not attempt to propose a new interpretation of wear mechanism but a way to compute experimental data and global models that already exist in the literature. At mesoscopic scale, our wear criterion, which is a threshold governing the mean surface $q_m(t)$, is discrete but at macro-scopic scale, the numerical model will be a representation of the continuous mechanism.

Now that we have interpreted all our parameters, we underline that Λ_α is the material loss rate. In the case of mild wear that is on discuss in this paper, this parameter has to be small compared to the geometry. It does mean that we can neglect Λ_α, which is the loss of height by period, in front of Λ_s, which is the height of the pattern. Then, the term $\mathcal{D}_\mathcal{L} - \mathcal{D}_w - \mathcal{D}_f$ can be neglected in front of $\mathcal{D}_w$, even if some wear dissipation are involved. It justifies *a posteriori* the wear criterion we chose.

9 CONCLUSIONS

In this paper, the local behavior of rubber-like material's surface in contact with a sliding indentor has been related to the wrinkled abrasion patterns observed. Hence, a mesoscopic scale model of mild wear phenomena has been introduced in order to derive macroscopic laws, compatible to a finite element model. The pattern has been seen a signature of wear, but not a quantification. We identified material and loading parameters on the only experimental mesoscopic easily accessible data, the geometrical features of abrasion patterns. A local wear criterion was introduced, based on energetic considerations. The whole model has exactly one local degree of freedom but can be identified to any phenomenological and global wear model. To illustrate the wear parameters indentification, we proposed two different identifications to a simple Thomas model, one for homogeneous wear, one for hertzian wear. The model will be complete after implementation in an numerical model, which is ongoing research.

REFERENCES

Archard, J. (1957). Elastic deformation and the laws of friction. *Proc. R. Soc. Ser. A. 243*, 190.

Fukahori, Y. and H. Yamazaki (1994). Mechanism of rubber abrasion. Part 2. general rule in abrasion pattern formation in rubber-like materials. *Wear 178*, 109–116.

Petitet, G. (2003). *Contribution à la compréhension des mécanismes élémentaires d'usure douce des élastomères chargés réticulés.* Phd these École Centrale, Lyon.

Reznikovskii, M. and G. Brodskii (1967). *Abrasion of rubber.* Maclaren Palmerton.

Schallamach, A. (1954). On the abrasion of rubber. *Proc. R. Soc. Ser. B. 67*, 883–891.

Stolz, C. (2003). *Energetic approaches in non-linear mechanics.* AMAS lectures Notes 11. Warsaw: Center of excellence for advanced materials and structures, IFTR, IPPT, Polish Acad. Sci.

Thomas, A. (1975). Factors influencing the strength of rubbers. *Rubber Chemistry and Technology 48*, 902–912.

Xia, F. (2003). Modelling of a two-dimensional coulomb friction oscillator. *Journal of Sound and Vibration 265*, 1063–1074.